Patterns of Dispersal and Dynamics among Habitat Patches Varying in Quality

Megan J. Donahue,[1,*] Marcel Holyoak,[2,†] and Charles Feng[3,‡]

1. Section of Evolution and Ecology, Graduate Group in Ecology, University of California, Davis, California 95616;
2. Department of Environmental Science and Policy, University of California, Davis, California 95616;
3. Mission San Jose High School, Fremont, California 94539

Submitted July 8, 2002; Accepted February 17, 2003; Electronically published September 5, 2003

ABSTRACT: Both source-sink theory and extensions of optimal foraging theory ("balanced dispersal" theory) address dispersal and population dynamics in landscapes where habitat patches vary in quality. However, studying dispersal mechanisms empirically has proven difficult, and dispersal is rarely tied back to long-term spatial dynamics. We used a manipulable laboratory system consisting of bacteria and protozoa to investigate the ability of source-sink and optimal foraging theories to explain both dispersal and emergent spatial dynamics. Consistent with source-sink models and contrary to balanced dispersal models, there was a consistent net flux of protist individuals from high to low resource patches. However, unlike the simplest source-sink models, intermediate rates of dispersal led to highest abundances in low resource patches. Side experiments found strong density dependence in local population dynamics and differences in average protist body size in high and low resource patches. Parameterization and analysis of a two-patch model showed that high migration from high to low resource patches could have depressed population density in low resource patches, creating pseudosinks. The movement of individuals and biomass from sources to sinks (a form of ecosystem subsidy) resulted in the convergence of body size and population densities in sources and sinks. Our results indicate a need to carefully consider movement patterns and interaction with local dynamics in potential source-sink systems.

Keywords: balanced dispersal, *Colpidium*, metapopulation, optimal foraging, source-sink, ecosystem subsidy.

* Corresponding author. Present address: Department of Biological Sciences, Dartmouth College, Hanover, New Hampshire 03755; e-mail: mjdonahue@ucdavis.edu.

† E-mail: maholyoak@ucdavis.edu.

‡ E-mail: cfeng@stanford.edu.

Am. Nat. 2003. Vol. 162, pp. 302–317. © 2003 by The University of Chicago. 0003-0147/2003/16203-020255$15.00. All rights reserved.

Habitat patches that vary in quality can cause population dynamics to differ between patches (Pulliam 1988). In such habitats, it has been difficult to predict patterns of between-patch movement (Diffendorfer 1998). It can be argued either that populations in better-quality patches are more productive and should produce more emigrants (Pulliam 1988) or, conversely, that optimally foraging individuals should leave good-quality habitats less frequently than poor-quality habitats (Fretwell and Lucas 1970; McPeek and Holt 1992). Tests of these opposing predictions have proven difficult because movement is infrequent and occurs over large spatial scales (e.g., Ims and Yoccoz 1996). In fact, of 47 empirical population dynamic studies with "source" and "sink" in the title or as keywords, only 13 (28%) contained any data on movement of organisms. Investigations of the ecological and evolutionary consequences of movement have been forced to use parsimonious general functions for dispersal (e.g., density-independent or density-dependent emigration). There is a need for more detailed investigations of interpatch movement and its influence on population dynamics in heterogeneous habitats.

Short-term and long-term patterns of movement may also differ because organisms may transport nutrients and other materials between patches, creating a form of ecosystem "subsidy" (Polis et al. 1997; Stapp et al. 1999). In the long term, such transport could change habitat quality, potentially altering within-patch population dynamics and subsequent patterns of between-patch dispersal. Despite this potential, the literature on spatial population dynamics and transport of materials has remained largely separate (see Nakano and Murakami 2001 for a notable exception). Here, we investigate both interpatch movement within generations and emergent spatial dynamics over hundreds of generations in habitats of varying patch quality. We start by briefly reviewing the relevant kinds of spatial dynamics.

Source-sink dynamics (Pulliam 1988) are the theoretical framework that is most frequently used to consider population dynamics in patches of varying quality. In coupled source-sink models, populations within patches are assumed to be at equilibrium, showing no net temporal

change in population size. A source is a compartment where births exceed deaths, giving a finite rate of increase (λ) greater than 1 and from which the excess individuals produced each generation emigrate (Pulliam 1988). Conversely, in a sink, deaths exceed births ($\lambda < 1$), and the population is prevented from declining by sufficiently regular arrival of immigrants from source populations. These definitions are for absolute sources and sinks. Alternatively, we may define relative sources and sinks as both having $\lambda > 1$ but with higher λ values for relative sources than relative sinks. In other systems, birth and death rates may be density dependent. For example, immigration may increase within-patch density and cause some otherwise viable ($\lambda \geq 1$) populations to show density-dependent reductions in the finite growth rate, resulting in $\lambda < 1$. These have been termed pseudosinks (Watkinson and Sutherland 1995). It is also possible that density dependence could reduce λ without causing λ to fall below unity. The effect of within-patch dynamics would be seen if dispersal were to cease, which would cause absolute sink populations to decline to extinction, relative sources and sinks to change in abundance but remain viable, and pseudosinks to return to viability. In all kinds of source-sink systems, predicting spatial patterns of population abundance is difficult because patterns result from the interaction of habitat quality, movement, and within-patch dynamics.

In the classic source-sink model (Pulliam 1988), all individuals that are in excess of the source's carrying capacity are assumed to emigrate from the source. Excess individuals have a greater survival rate in the sink than if they remained in the source. Therefore, regional population size (including both source and sink patches) is enhanced by migration from the source to the sink and is largest when source to sink dispersal rates are highest. By contrast, in some source-sink models, intermediate dispersal rates produce the largest regional population size, since very high migration rates can reduce the source below carrying capacity, resulting in a decline in population growth rate and hence the regional population (Wootton and Bell 1992; Doak 1995; Delibes et al. 2001).

Source-sink models usually assume simple formalisms for net movement from sources to sinks. Either a constant (density-independent) proportion of individuals emigrate per generation (e.g., Howe et al. 1991) or a simple density-dependent function operates, such as emigration of all offspring in excess of the source's carrying capacity (e.g., Pulliam 1988). By contrast, optimal foraging models assume that individuals will distribute themselves to maximize their fitness (Fretwell and Lucas 1970). In patches with different carrying capacities and a density-independent per capita rate of emigration, this is predicted to cause emigration to evolve to become inversely proportional to the carrying capacity of that patch (McPeek and Holt 1992). This "balanced dispersal" (McPeek and Holt 1992) results in a balance in the number of individuals moving in each direction, creating no net between-patch flux of individuals. By contrast, source-sink models predict that net movement of individuals is from a source to a sink (Diffendorfer 1998).

The mechanisms of dispersal in real populations have remained obscure because movement is difficult to quantify (Ims and Yoccoz 1996). Simple density-independent models of individual movement behavior (correlated random walks) predict that dispersal rates for whole populations should be highly variable, making it difficult to test for movement processes and the functional forms for dispersal (Cain 1991). Instead, in reviewing 28 cases in the literature, Diffendorfer (1998) used simplified criteria to distinguish source-sink models (unidirectional dispersal and $\lambda < 1$) and balanced dispersal models (no net directionality to movement and low carrying capacities). Even with these simplified criteria, there was insufficient evidence about the fit to these two models in all cases. Diffendorfer (1998) also did not consider pseudosinks, making assessments of source versus sink status unreliable (Watkinson and Sutherland 1995).

Over time, all habitat patches vary in quality, and it is possible that sources and sinks will undergo inversions, where sources become sinks and vice versa (e.g., Pulliam 1996). There are a wide variety of reasons why inversions might occur. First, source versus sink status may be dynamic; for example, habitat quality might change with succession (Pulliam 1996) or degradation (Doak 1995), or pseudosinks may be changed into sources by changes in patch occupancy (Boughton 1999). Second, source-sink inversions could result from evolution (Dias 1996). Adaptation to sink conditions might be hindered by gene flow from sources, and temporal changes in the relative frequency of source and sink populations (as local adaptation proceeds) may alter rates of gene flow to sink habitats, thereby influencing the potential for source-sink inversions (Dias 1996). Finally, sinks might be transformed into sources by "subsidy" (Polis et al. 1997), which is when a donor-controlled resource (prey, detritus, or nutrients) is transported from one habitat to another, where it is consumed; for example, salmon die after spawning, bringing large amounts of energy and nutrients to nutrient-poor headwater streams (reviewed by Polis et al. 1997). If transported materials accumulate, subsidy could cause source-sink inversions. Traditionally, subsidy involves transport between different ecosystems (Polis et al. 1997), whereas here we are interested in the effects of transport among patches of different quality.

We investigated a manipulable laboratory microcosm system consisting of decomposing seeds and nutrient medium that are consumed by bacteria, which in turn are

consumed by a ciliated protist, *Colpidium striatum* Stokes. This protist has a generation time of about 5 h (Holyoak and Lawler 1996*a*) so that a large amount of information about population dynamics can be obtained quickly. Conducting a study in microcosms allowed us to obtain information about long-term dynamics and net rates of movement of individuals and biomass; such information would be difficult to obtain in the field. We used this system to ask two related questions: First, is there a net movement of individuals from sources to sinks, or do equal numbers of individuals move in both directions, as predicted by models of balanced dispersal and optimal foraging? Second, is there feedback between the movement of *C. striatum* and long-term population dynamics? If so, is this related to the movement of resources (a form of subsidy), or is it a direct response to changes in local population density?

We report a series of six experimental and modeling studies. In the perturbation experiment, we assessed the potential relevance of pseudosink theory. This experiment used density perturbations and model fitting to quantify density dependence in isolated local (patch) populations. In the dispersal experiment, we measured rates of *C. striatum* dispersal. In the spatial dynamics experiment, we constructed microcosms with a patchy distribution of resources and three different levels of dispersal (fig. 1). To obtain a record of spatial and temporal distribution, *C. striatum* densities were sampled from each patch every 2 d for at least 36 d (166 *C. striatum* generations). To investigate the relevance of subsidy, we looked at changes in *C. striatum* body size with resource levels and movement. We assessed the relevance of source-sink (and pseudosink) and balanced dispersal models using estimates of net movement between patches; this involved using densities from the spatial dynamics experiment and per capita movement rates from the dispersal experiment. Finally, we used a model of spatial dynamics to ask whether the observed fluxes in individuals or biomass and potential mechanisms of source-sink or pseudosink dynamics were capable of causing the long-term dynamics observed in the spatial dynamics experiment. Altogether, these analyses uniquely synthesize the role of different branches of ecological theory for predicting movement and dynamics in systems with patchy resources.

Study Organisms

Colpidium striatum is a free-swimming ciliated protozoan that is commonly found in freshwater. When food is plentiful, ciliates have a fixed time between divisions, which is the length of the cell cycle (biomass accumulation and mitosis or meiosis; Finlay 1977). *Colpidium striatum* were

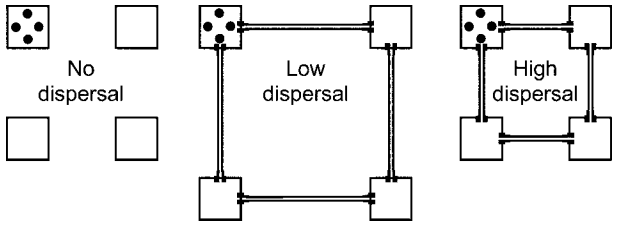

Figure 1: Treatments in the spatial dynamics experiment. Squares indicate 32-mL bottles, which are connected by tubes in some treatments. Solid circles represent wheat seeds.

grown on a mixed flora of common freshwater bacteria, *Serratia marcescens* Bizio, *Enterobacter aerogenes* Hormaeche and Edwards, and *Bacillus subtilus* var. *niger* (Ehrenberg) Cohn. All study organisms were obtained from Carolina Biological Supply (Burlington, N.C.). Nutrients were supplied using wheat seeds and a dilute plant-based medium.

Kaunzinger and Morin (1998) showed that *C. striatum* reduced bacteria (*S. marcescens*) to a predictable and relatively constant abundance regardless of the strength of the nutrient medium. Their result accords with the Monod (1950) model where resources (in this case, bacteria) are grazed down to an equilibrium level, R^* (Tilman 1977, 1982). In the absence of dispersal and over long time periods, densities of *C. striatum* should reflect nutrient availability. A simple mechanism also links cell size with changes in nutrient level: protists like *C. striatum* have a cell cycle of a constant duration at a given temperature (Finlay 1977), and a greater density of nutrients provides more bacteria at equilibrium (Kaunzinger and Morin 1998), which should allow protists to become larger between divisions; manipulations of either liquid nutrient concentrations or seeds confirm this expectation (M. Holyoak, unpublished data).

To initiate cultures, a dilute nutrient medium was made by adding 0.1 g of crushed Protozoan Pellet (Carolina Biological Supply) and 0.1 g of Herptivite multivitamin powder (Rep-Cal Research Labs, Los Gatos, Calif.) to 1 L of spring water, steam autoclaving, cooling, and then pouring off the supernatant into a sterile flask. A standardized bacterial solution was made by adding 5 mL of a liquid stock culture of the three bacterial species to 1 L of dilute nutrient medium. After 24 h, 30 mL of bacterial solution was placed into each of the 32-mL polypropylene bottles (patches) with either zero (low resource patch) or four (high resource patch) wheat seeds. Each bottle was inoculated with 0.5 mL of *C. striatum* to give approximately 15 cells/mL in every bottle. This culturing method was used in all experiments.

In the dispersal experiment and the spatial dynamics

experiment, there were three dispersal treatments (fig. 1): no, low, or high dispersal. Distances between adjacent bottles were 7.2 cm and 12.2 cm, respectively, in high and low dispersal microcosms. Of the 30 mL of solution placed into each bottle, tubes contained 1.0 mL (3.3%) in high dispersal microcosms and 1.51 mL (5%) in low dispersal microcosms. Wall surface area inevitably differs between high and low dispersal microcosms. However, *C. striatum* feeds mainly in the water column and was not influenced by wall area in previous experiments (Holyoak and Lawler 1996*a*, 1996*b*). In all experiments, sampling procedures for *C. striatum* were similar to those of Holyoak (2000).

Perturbation Experiment: Testing for Density Dependence in Local Populations

Methods

To ascertain the presence and strength of density dependence in local dynamics, we tested the fit of a density-dependent model to data from a perturbation experiment. In the experiment, we perturbed *Colpidium striatum* populations above and below carrying capacity, counted protists (N_t) immediately after this perturbation, and counted again after 12 h (N_{t+1}).

Colpidium striatum were raised in the manner described above. After 6 d (approximately 24 generations), when the local populations had reached carrying capacity, we performed the perturbations. The contents of each bottle were poured into tubes and centrifuged for 7 min at 1,000 rpm. The supernatant was pipetted back into the original bottle, and some percentage of the *C. striatum*–rich centrifugate was returned to the bottle: 0%, 25%, 50%, or 100% for downward or no perturbations and 150%, 200%, 300%, or 400% for upward perturbations. Extra populations were raised and centrifuged to provide extra centrifugate for upward perturbations. We performed three replicate perturbations of each percentage on each of 2 d. Samples from each of these populations were counted immediately after the perturbation and again after 12 h.

After preliminary analyses to select an appropriate population model, we assessed the fit of the Beverton and Holt (1957) model to the data. The Beverton-Holt model is a solution to the logistic model and can be thought of as the logistic sampled in discrete time. Using a likelihood approach, we jointly fit the zero-seed and four-seed perturbation data to compare models in which R_i, the maximum growth rate and/or a_i, a parameter inversely related to the carrying capacity, were allowed to vary by seed level, i:

$$N_{i,t+1} = \frac{R_i N_{i,t}}{1 + a_i N_{i,t}}. \quad (1)$$

The four models were log-transformed (to give $\ln N_{i,t+1} = \ln R_i + \ln N_{i,t} - \ln [1 + a_i N_{i,t}]$) and fit with lognormal process error. We found the most parsimonious model with likelihood ratio tests (LRT) for nested models and Akaike Information Criterion (AIC) for nonnested models (see Hilborn and Mangel 1997 for an introduction to these methods; Burnham and Anderson 1998). Bootstrapping was used to generate confidence intervals for the parameters.

Since population dynamics in the microcosms proceed in continuous time, we estimated the strength of density dependence in a form that is consistent with continuous time dynamics. We did this by back transforming parameters from the Beverton-Holt model to those for the logistic equation, such that $r = \ln(R)/\Delta t$ and $K = (R - 1)/a$, where Δt is 12 h in the perturbation experiment. The strength of density dependence was defined as the change in the per capita population growth rate caused by a unit change in population size N_i; this is the slope (derivative) of the per capita growth rate. The per capita growth rate is $1/N\ dN/dt$, and its derivative is $-r/K$.

Results

Density dependence was present in local dynamics in both zero- and four-seed bottles (fig. 2). The most parsimonious model was one in which R took a single value but a varied by seed level. This model fit significantly better than a model with the same a and R for both seed levels (LRT, $P = .00008$) and was more parsimonious than a model fitting separate a's and R's for each seed level (LRT, $P = .364$). The model that allowed only R to vary between seed levels had a $\Delta\text{AIC} = 5.26$, indicating less support for that model compared to the most parsimonious model. Maximum likelihood parameters and bootstrapped 95% confidence intervals for the most parsimonious model were $R = 1.60$ (1.35, 2.00); $a_0 = 0.00051$ (0.00026, 0.00082); and $a_4 = 0.00024$ (0.00014, 0.00036; fig. 2). Density dependence was estimated to be stronger (strength is defined in "Methods") in zero-seed bottles ($-r/K_0 = -3.36 \times 10^{-5}$ h^{-1} mL than in four-seed bottles: $-r/K_4 = -1.59 \times 10^{-5}$ h^{-1} mL).

Dispersal Experiment

Methods

We measured dispersal rate as the proportion of *Colpidium striatum* undergoing unidirectional movement from a bottle containing bacteria and *C. striatum* (the donor bottle) to an adjacent bottle containing only bacteria (the receiving bottle). For both zero- and four-seed treatments, six pairs of bottles were connected with short tubes and six pairs with long tubes. We created a range of densities in

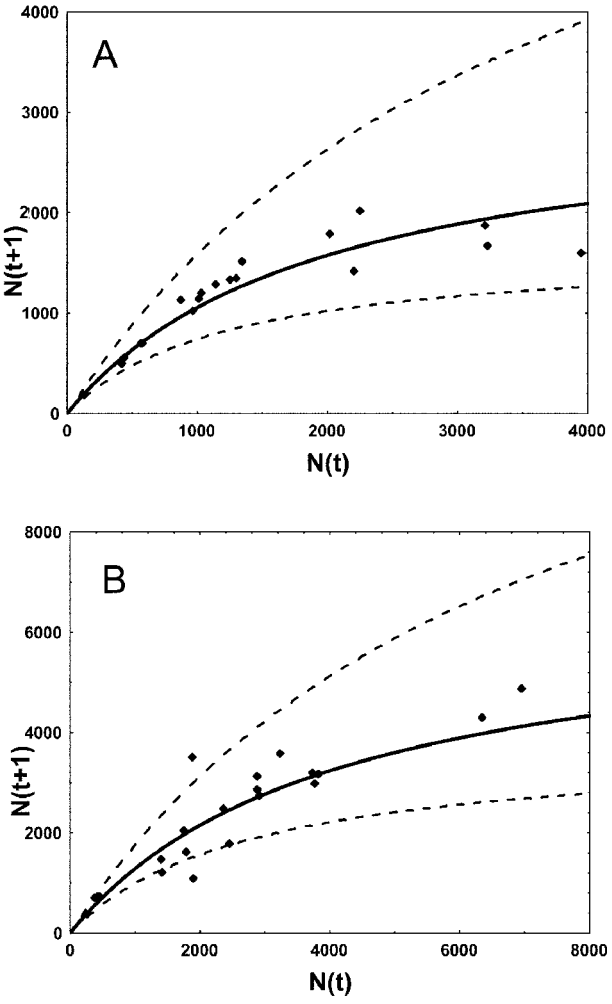

Figure 2: The fit of the most parsimonious Beverton and Holt (1957) model to data from the perturbation experiment for bottles with zero seeds (*A*) or four seeds (*B*). Solid lines show the fitted curves, and dashed lines show bootstrapped 95% confidence limits. This model allows *a* to vary between seed levels, while *R* remains the same for both seed levels.

the donor bottles for both zero- and four-seed populations using centrifugation. Due to time constraints, the experiment was blocked across 3 d. The tube of each microcosm was clamped off, and each donor population (after density perturbation) was randomly assigned to a microcosm. Each receiving bottle was filled with 30 mL of standardized 7-d-old bacterial solution with no seeds. The experiment was initiated by releasing the clamp on the tube. After 2 h, *C. striatum* density was sampled in all bottles; this allowed calculation of both the initial *C. striatum* density and the proportion dispersing per generation.

Results

The *C. striatum* emigration rate from high dispersal (short-tube) bottles was on average 57% greater than from low dispersal (long-tube) bottles, but this difference was not statistically significant (tables 1, 2). In fact, no effects of day (=block), seed number, or dispersal treatments were significant either as main effects or interactions (table 2). The broad 95% confidence limits in table 1 indicate that dispersal was enormously variable among replicates.

Tests for density dependence using regressions of arcsine–square root–transformed proportions dispersing revealed no evidence for density dependence at $P < .05$. Additionally, slopes indicated by T values in table 1 were a mixture of positive and negative values, indicating that there was no single mechanism for any undetected density dependence. Power tests in table 1 are consistent with there being weak power (0.09–0.21) to detect small effects ($R^2 = 0.02$; Cohen 1988) but high power (0.63–0.998) for detecting large effects ($R^2 = 0.26$; Cohen 1988). Given that we conducted four independent or seven semi-independent tests (table 1), it is likely that density dependence in dispersal is either very weak (low R^2 values) or absent.

Spatial Dynamics Experiment

Methods

Three replicates of each of three types of microcosms were constructed: no, low, or high dispersal (fig. 1). Microcosms were assembled and sterilized with four wheat seeds in one bottle and zero seeds in the other bottles. Each bottle was filled with 30 mL of bacteria culture and inoculated with *Colpidium striatum* 24 h later, using the procedures described above.

Starting 3 d later, samples were taken every 2 d for 36–40 d, depending on the treatment (fig. 3). Samples of 3 mL were taken from individual bottles after tightening bottle caps to create an air lock that minimized between-bottle flow. Samples were replaced with fresh, sterile, dilute nutrient medium, which created a semicontinuous batch culture. All microcosms were kept at room temperature (mean = 23°C, standard deviation = 0.7°C from 21 measurements). One of the high dispersal microcosms was excluded from all analyses because of contamination with fungi.

Statistical analyses only used 36 d, which were available from all treatments. *C. striatum* would have reached equilibrium densities within the 72 h between setup and the first sample (Holyoak and Lawler 1996*a*). Densities were calculated from individual microcosm bottles with zero or four seeds, and average densities were calculated from entire microcosms. Temporal trends in density were assessed

Table 1: Results of dispersal experiment, regressions of arcsine (square root of proportion that dispersed) versus ln (donor density/*K*) for particular seed- and tube-length treatments

			% dispersing per generation (~5 h)		Regression results			Power	
Seeds	Dispersal	*n*	Mean[a] (%)	95% CI[a]	T[b]	P	R^2	Small effect	Large effect
0	Low	17	.214	.229–1.96	−2.11	.052	.23	.09	.63
0	High	18	.282	.162–2.14	1.60	.13	.14	.09	.65
4	Low	18	.156	.047–1.01	−.51	.61	.016	.09	.65
4	High	17	.335	.205–2.58	−.19	.85	.0024	.09	.63
0 or 4	Low	35	.183	.124–1.45	−1.80	.081	.089	.13	.92
0 or 4	High	35	.307	.172–2.31	.92	.36	.025	.13	.92
0 or 4	Low or high	70	.241	.153–1.89	−.38	.70	.002	.21	.998

Note: These values are percentages (e.g., .214% is a .00214 probability of dispersing). Power is the power to detect a small difference (coefficient of determination, $R^2 = 0.02$) or large difference ($R^2 = 0.26$; Cohen 1988) with α of 0.05 performed using a post hoc test in G*Power Statistical Software. Additional regressions not in the table used ln (donor density) instead of ln (donor density/*K*); however, this did not cause any regression to become significant at $P < .05$.

[a] Back transformed from arcsine–square root proportions and based on a generation time from Holyoak and Lawler (1996*a*).

[b] df = $n - 2$.

using linear regression of ln (density + 1) against day number. The confidence measures on slopes and intercepts from individual microcosms or bottles are unreliable because of temporal autocorrelation (e.g., Dennis and Taper 1994). This problem was avoided by using microcosms as the unit of replication, so that microcosm means for slopes and intercepts were used in statistical tests (and standard errors of individual slopes or intercepts were ignored). Parametric tests were used unless data were nonnormal or variances were heterogeneous.

Results

Population declines are common in microcosms that are not chemostats, and we see such declines in our results (fig. 3). The slow release of nutrients from seeds and the pulsed input of small amounts of nutrient medium are not sufficient to balance population samples and losses from respiration. However, the decline in population densities is slow relative to the *C. striatum* generation time. Averaged across all patches within a microcosm, protist densities declined more rapidly in no or high dispersal microcosms than in low dispersal microcosms (fig. 3; table 3; using a median test because of heteroscedasticity, $\chi^2_2 = 6.34$, $P < .05$). Analysis of changes in densities within individual bottles (patches) showed that densities in patches without seeds declined more rapidly in microcosms with high or no dispersal than with low dispersal (fig. 3; table 3; median test, $\chi^2_2 = 6.21$, $P < .05$). However, densities declined at a similar rate in bottles with four seeds regardless of the level of dispersal (table 3; median test, $\chi^2_2 = 0.67$, $P \approx .7$).

Since both initial densities and rates of declines differed, we also looked directly at time-averaged *C. striatum* densities. Densities in entire microcosms were significantly higher with low dispersal than with no or high dispersal (fig. 4; one-way ANOVA on ln [density + 1]-transformed values for microcosm averages, $F = 45.9$, df = 2, 5, $P < .001$). Mean density was greater in low dispersal microcosms than in either no dispersal ($P < .001$) or high dispersal microcosms ($P < .001$), which did not differ significantly from each other (fig. 4). Comparisons of densities in individual microcosm bottles suggested that this difference was due to zero-seed bottles and not four-seed bottles; the average density in patches with zero seeds was significantly higher with low dispersal than high or no dispersal, whereas there were no significant differences in mean density in four-seed bottles of different dispersal treatments (fig. 4). Power tests indicated that the power to detect a difference in mean densities with dispersal in one-way ANOVAs was high (>0.99) for the observed differences in means in zero-seed bottles but low (0.11) for four-seed bottles.

The net effect of low dispersal rates was that average *C.*

Table 2: ANOVA from the dispersal experiment with arcsine (square root of proportion that dispersed) as the dependent variable and day (1, 2, or 3), number of seeds (0 or 4), and dispersal treatment (short or long tubes) as factors

Source	df	MS	F	P
Day	2	1.628×10^{-3}	1.89	.160
Seeds	1	$.002 \times 10^{-3}$	2.47×10^{-3}	.961
Dispersal	1	1.203×10^{-3}	1.40	.242
Day × seeds	2	$.186 \times 10^{-3}$	.218	.806
Day × dispersal	2	$.091 \times 10^{-3}$	.105	.900
Seeds × dispersal	1	$.250 \times 10^{-3}$	.290	.592
Day × seeds × dispersal	2	$.384 \times 10^{-3}$	.447	.642
Error	58	$.860 \times 10^{-3}$	…	…

striatum densities in zero- and four-seed bottles became more similar to each other (fig. 4). Without dispersal, *C. striatum* density was ~9.0 times greater with four seeds than with no seeds compared to only 2.6 times with low dispersal; this difference in ratios was significant in a Mann-Whitney *U*-test ($Z = 1.96$, $P < .05$, $n = 6$ microcosms). High dispersal produced differences in density between zero- and four-seed bottles of 11.1 times, which were similar to the ratio with no dispersal ($Z = 0.577$, $P \approx .6$ in a Mann-Whitney *U*-test, $n = 5$ microcosms).

Body Size

Methods

On day 34 of the spatial dynamics experiment (day 30 for low dispersal microcosms), we measured the volumes of 30 *Colpidium striatum* cells from the 3-mL samples. Measurements were made for every four-seed bottle and selected zero-seed bottles; we gained no further understanding by considering all zero-seed bottles. For low and high dispersal microcosms, the selected zero-seed bottle was adjacent to a four-seed bottle. For no dispersal microcosms, it was a randomly selected zero-seed bottle. Cells were killed using Lugol's iodine solution at a final concentration of 0.4%. This caused cell volumes to shrink by ~13% relative to live cells, but small and large cells shrank by similar amounts; uncorrected cell measurements were used to calculate cell volumes.

Dark field illumination under a binocular microscope at 15× magnification and a monochrome video image analysis system (resolution 640 × 480 pixels) were used to measure protist length ($2 \times \alpha$) and greatest width ($2 \times \beta$); pixel size was calibrated using a stage micrometer. Following Hewett (1980), volumes of cells (v) were calculated using the formula for a prolate spheroid (an ellipse rotated around the major axis), which is $v = 4\pi\alpha\beta^2/3$. We used MANOVA to test the effect of dispersal on ln (mean cell volume) from zero-seed and four-seed bottles.

Results

After 30 d, *C. striatum* cells were larger in isolated bottles with four seeds (mean $= 4.83 \times 10^4\ \mu m^3$) than in bottles with no seeds (mean $= 1.37 \times 10^4\ \mu m^3$; fig. 5*A*). Dispersal increased mean cell volume in bottles without seeds but decreased cell volume in bottles with four seeds (overall, Wilks's $\lambda_{6,6} = 0.014$, $P < .02$; for zero-seed bottles $F = 16.1$, df $= 3, 4$, $P < .01$ and for four-seed bottles $F = 7.43$, df $= 3, 4$, $P < .05$). Mean cell volumes did not differ ($P = .5$ and $P = .8$, respectively) between high and low dispersal bottles with either zero or four seeds (fig. 5*A*). The effect of dispersal on cell volume was strong enough that mean volumes also did not differ ($P = .5$) between zero- and four-seed bottles in microcosms that permitted dispersal (fig. 5*A*).

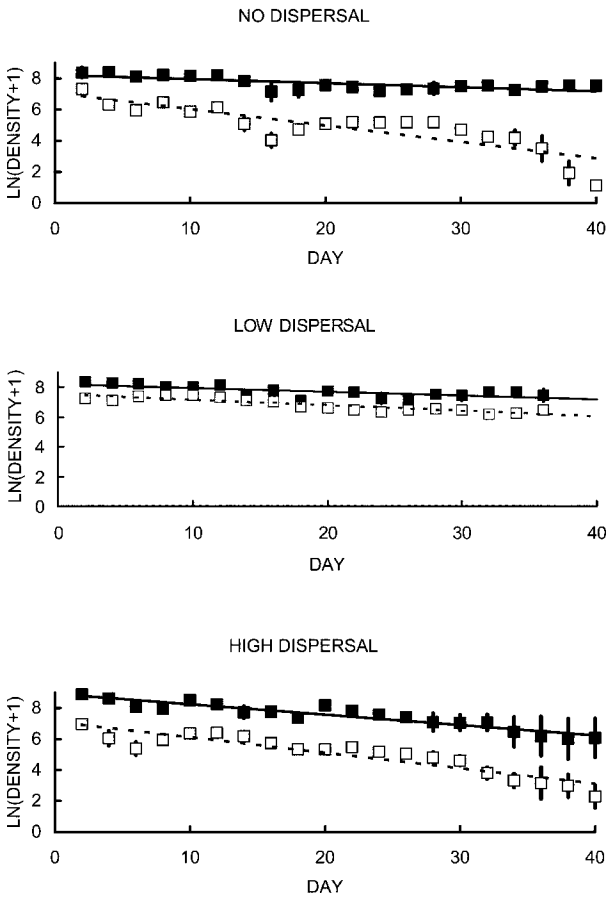

Figure 3: Mean *Colpidium striatum* densities through time in microcosms with no, low, or high dispersal. Solid squares indicate bottles with four seeds, and open squares indicate bottles without seeds. Straight lines indicate linear regressions of ln (1 + cells per mL) versus day number using only days 2–36; solid lines for four-seed bottles and dashed lines for zero-seed bottles. Each point is the average for bottles of a given type with standard error bars coming from microcosm means ($n = 3$ for no or low dispersal, $n = 2$ for high dispersal) that were first calculated separately for each bottle type for each day within a microcosm.

These dispersal effects were unlikely to have been directly caused by the mixing of small and large cells from different bottles because the standard deviation of cell volumes showed no large increases with dispersal (fig. 5*B*). The only differences were a large decrease in variability in cell size in zero-seed bottles with low dispersal compared to no dispersal and a small increase in variability with dispersal in four-seed bottles (fig. 5*B*). Preliminary experiments also showed that cells rapidly changed in size when moved between nutrient mediums of different con-

centrations; large cells divided into a number of smaller cells when placed in lower quality mediums and small cells rapidly grew in average volume when placed in higher quality mediums.

Estimates of Net Movement

Methods

Net movement of *Colpidium striatum* in the spatial dynamics experiment was estimated using the mean dispersal rate from the dispersal experiment. Movement was calculated using fluxes in either individuals or protist biomass. Both measures assume that movement is density independent (tables 1, 2). Let $N_{i,t}$ be the number of *C. striatum* in bottle i at time t ($i = a, b, c$, where bottle b is adjacent to bottles a and c), and let p_i be the proportion of individuals leaving a bottle in the dispersal experiment with the seed number and tube length corresponding to bottle i. Each measure was calculated based on the density, $N_{i,t}$, for three periods in the spatial dynamics experiment: initial ($t = 0$), final ($t = 36$), and mean ($t = 0$–36). Net individual migration $M1 = N_{a,t}p_a + N_{c,t}p_c - 2N_{b,t}p_b$ is the net number of individuals entering or leaving a patch per generation. Net biomass movement $M2 = V_{a,t}N_{a,t}p_a + V_{c,t}N_{c,t}p_c - 2V_{b,t}N_{b,t}p_b$ is the absolute biomass of material transported between patches per generation, where $V_{i,t}$ is the mean volume of protist cells for bottle i at time t. "Initial" calculations used mean *C. striatum* cell volumes from no dispersal microcosms, representing the condition before dispersal could have acted. "Mean" and "final" conditions used cell volumes from dispersal treatments on day 34 of the spatial dynamics experiment (day 30 for low dispersal microcosms); this represented conditions after dispersal had potentially altered protist cell volumes.

Table 3: Results of linear regressions showing temporal trends in ln (density + 1)

Dispersal	Intercept (SE)	Slope (SE)
Microcosm average:		
None	7.07 (.15)	−.0631 (.009)
Low	7.69 (.29)	−.0346 (.008)
High	7.43 (.48)	−.0816 (.029)
Bottles with four seeds:		
None	8.32 (.18)	−.0327 (.010)
Low	8.23 (.01)	−.0267 (.007)
High	8.84 (.45)	−.0617 (.034)
Bottles with zero seeds:		
None	6.59 (.17)	−.0680 (.009)
Low	7.51 (.10)	−.0373 (.003)
High	6.96 (.49)	−.0882 (.027)

Note: For each bottle type, the table gives the mean values of the intercept and slope from regressions conducted separately for each bottle; intercept and slope values were first averaged within microcosms and then, to avoid pseudoreplication, microcosm means were used to calculate the values given. Microcosm average values were from a single regression for the average ln (density + 1) series from each microcosm, which were then averaged to give the value in the table. Standard errors (SE) were calculated using microcosms as the unit of replication; therefore, $n = 2$ for high dispersal and $n = 3$ for low or no dispersal.

Results

Net individual migration, $M1$, was estimated in the spatial dynamics experiment to show a net flow from four-seed to zero-seed bottles in both low and high dispersal microcosms. This remained the case whether initial, mean,

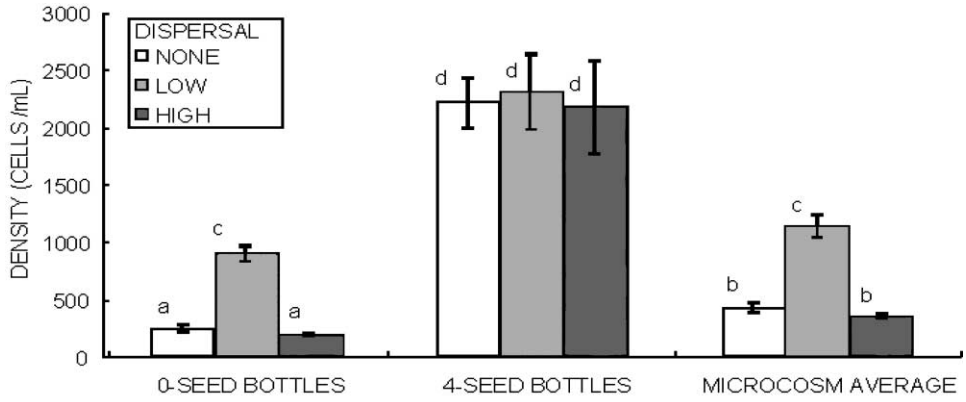

Figure 4: Average *Colpidium striatum* densities from days 2–36 in bottles with zero seeds, four seeds, or the average from entire microcosms and with no, low, or high dispersal. Error bars show standard errors. Bars with the same letters above them did not differ (at $P < .05$) in least significant difference tests. One-way ANOVAs with dispersal level as a factor gave $F = 35.9$, df = 2, 5, $P = .001$ for zero-seed bottles and $F = 0.38$, df = 2, 5, $P = .70$ for four-seed bottles.

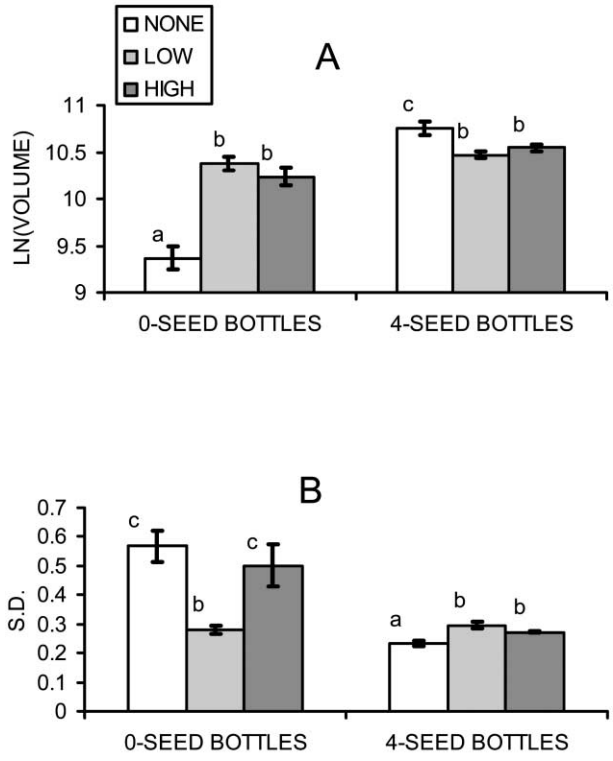

Figure 5: *A*, Mean volumes (μm^3) and, *B*, standard deviations (SD) of ln (volume) of *Colpidium striatum* cells from bottles with either zero or four seeds and different levels of dispersal on day 34 of the spatial dynamics experiment. Each bar is the average (and standard error) from microcosm averages for each type of bottle ($n = 3$ microcosms for no or low dispersal and $n = 2$ microcosms for high dispersal). Bars with the same letters above them did not differ (at $P < .05$) in least significant difference tests.

or final *C. striatum* densities were used (fig. 6*A*). At the start of the experiment, *M*1 was 2.8 times greater for high dispersal microcosms than low dispersal, but this difference declined to 1.2 times by the end of the experiment (fig. 6*A*) because of declines in density (fig. 3). Regardless of the point in the experiment that calculations were made, there was an estimated net loss of *C. striatum* biomass (*M*2) from four-seed bottles with high or low dispersal (fig. 6*B*). Like *M*1, differences in *M*2 between low and high dispersal treatments also diminished through the experiment (fig. 6*B*) because of greater declines in cell densities in high dispersal microcosms (fig. 3).

A Model of Spatial Dynamics

Methods

Using the maximum likelihood estimates (MLE's) for R, a_0, and a_4 from the perturbation experiment, we simulated the dynamics in our experiment by connecting two patches with Beverton-Holt dynamics over a range of dispersal rates (m_{ij}):

$$N_{0,t+1} = (1 - m_{04})\frac{RN_{0,t}}{1 + a_0 N_{0,t}} + m_{40}\frac{RN_{4,t}}{1 + a_4 N_{4,t}}, \quad (2a)$$

$$N_{4,t+1} = (1 - m_{40})\frac{RN_{4,t}}{1 + a_4 N_{4,t}} + m_{04}\frac{RN_{0,t}}{1 + a_0 N_{0,t}}, \quad (2b)$$

where $N_{i,t}$ is population density in a bottle with i seeds at time t, m_{04} is the per capita migration rate from bottles with zero seeds to bottles with four seeds, and m_{40} is the per capita migration rate from bottles with four seeds to bottles with zero seeds; other parameters are as in equation (1). The migration parameters were adjusted to a 12-h time step to match the parameters from the perturbation experiment. This is the same model as used by Watkinson and Sutherland (1995). Simulations with two and four patches (arranged as in the spatial dynamics experiment) gave qualitatively similar results for our parameter values; for ease of presentation, we present only the two-patch model.

To incorporate the differences in body size between zero- and four-seed bottles (fig. 5), we used the ratio of cell volumes in bottles i and j (v_i and v_j) to adjust the dispersal rates:

$$N_{i,t+1} = (1 - m_{ij})\frac{RN_{i,t}}{1 + a_i N_{i,t}} + \left(\frac{v_j}{v_i}\right)m_{ji}\frac{RN_{j,t}}{1 + a_j N_{j,t}}. \quad (3)$$

Since cells in four-seed, no dispersal bottles grew approximately three times larger than in zero-seed bottles, this adjustment triples the dispersal rates from four- to zero-seed bottles and decreases to one-third the dispersal from zero- to four-seed bottles. With this adjustment, the model tracks the population in each bottle in terms of local biomass units (the local average size of cells, which is different for different bottles) instead of direct individual counts. We chose this formalism to better account for the possible effects of nutrient movement by individual dispersal or the differing reproductive potential of different-sized individuals.

To account for observed declines in population density over time, we further modified equation (3) by including either exponential decline in carrying capacity (eq. [4a]) or in patch growth rate, λ (eq. [4b]), transformed to discrete time:

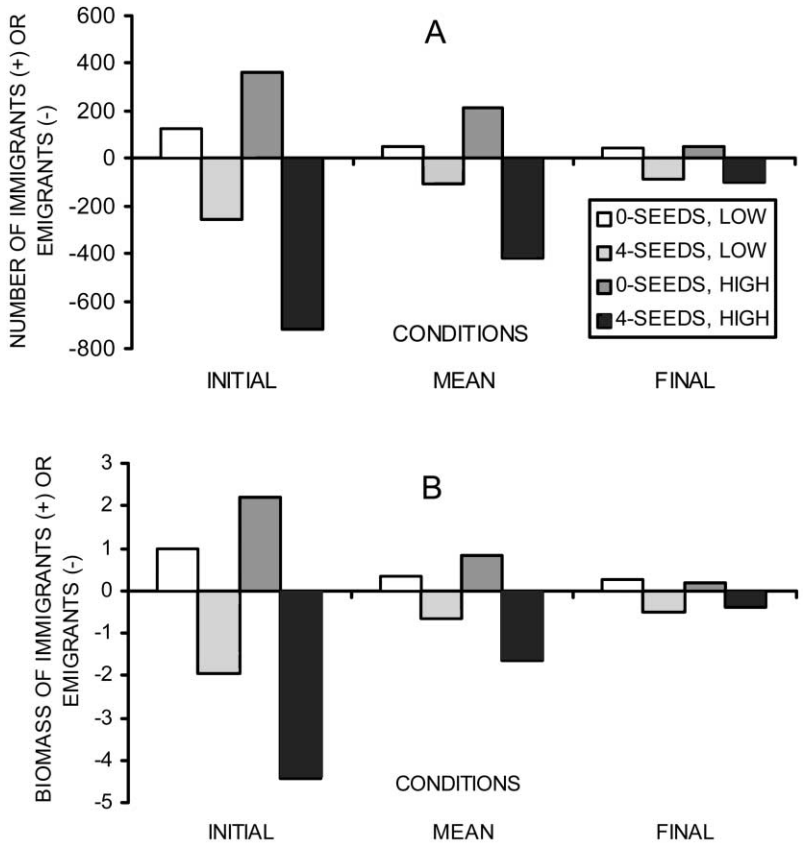

Figure 6: Two alternative measures of net movement per generation. Positive values indicate a net influx, and negative values indicate a net loss. White bars represent zero-seed bottles in low dispersal microcosms; light gray, four-seed bottles in low dispersal microcosms; dark gray, zero-seed bottles in high dispersal microcosms; and black, four-seed bottles in high dispersal microcosms. *A*, Total number of individuals moving, M_1. *B*, Net movement of *Colpidium striatum* biomass in $\mu m^3 \times 10^7$, M_2. Calculations for zero-seed bottles used bottles that were adjacent to four-seed bottles. Calculations were made for initial conditions ($t = 0$ d), final conditions ($t = 36$ d), and mean conditions ($t = 0$ to 36 d); in the latter case, $N_{i,t}$ was the average number of cells between days 0 and 36.

$$N_{i,t+1} = (1 - m_{ij})\frac{RN_{i,t}}{1 + a_i e^{k_i t} N_{i,t}} + \left(\frac{v_j}{v_i}\right) m_{ji} \frac{RN_{j,t}}{1 + a_j e^{k_j t} N_{j,t}}, \quad (4a)$$

$$N_{i,t+1} = (1 - m_{ij})\frac{RN_{i,t}}{1 + a_i N_{i,t}} e^{-k_i t} + \left(\frac{v_j}{v_i}\right) m_{ji} \frac{RN_{j,t}}{1 + a_j N_{j,t}} e^{-k_j t}. \quad (4b)$$

Using the MLEs of R, a_0, and a_4 (see perturbation experiment), we fit the decline parameters k_0 or k_4 in each of these models to the zero-seed or four-seed no dispersal dynamics from the spatial dynamics experiment. To find the MLEs for k_0 and k_4, we used one-step-ahead predictions and lognormally distributed process error; we bootstrapped confidence intervals for the MLE-selected model.

We simulated two-patch model dynamics using only the basic model (eqq. [2a], [2b]), including body size effects (eq. [3]), including only population decline (eqq. [2a], [2b] plus exponential decline), or including both body size effects and population decline (eqq. [4a], [4b]). In all cases, we present the time-averaged densities from zero- or four-seed patches for simulations of the same duration as the spatial dynamics experiment. For simplicity, we present results for cases where per capita movement rates were equal ($m_{04} = m_{40}$), which is consistent with the results of the dispersal experiment; considering asymmetric dispersal rates did not improve our understanding of the problem. We also note that, as reported in the results for the spatial dynamics experiment, we could make only weak inferences about long-term

changes in average density with dispersal in four-seed bottles because of low statistical power.

Results

The simple two-patch model (eqq. [2a], [2b]) with MLE values for parameters resulted in stable population sizes. Average population densities in the zero-seed bottle increase monotonically with dispersal rate (fig. 7*A*, *solid line*); observed declines in population density with increasing dispersal (fig. 4) were not predicted by the model. However, increasing the parameter differences between the patches ($a_0 = a_0 + 2\sigma_{a0}$, $a_4 = a_4 - 2\sigma_{a4}$, where σ is estimated from the bootstrapping in the perturbation experiment) resulted in zero-seed bottle densities being slightly higher at intermediate dispersal rates (fig. 7*A*, *dashed line*).

Adjusting dispersal for differences in cell size has two effects compared to equations (2a) and (2b): increasing the size of the zero-seed average density and causing population densities in the zero-seed bottle to become greatest at intermediate dispersal rates, m_{40} and m_{04} (fig. 7*A*, *dotted line*). Increasing the differences between patches enhanced this effect (fig. 7*A*, *dashed-dotted line*). However, dispersal rates producing declines in zero-seed average density were much greater than those in the dispersal experiment; the relevant per capita rates of dispersal for interpreting figure 7 (with a 12-h time step to accord with the perturbation experiment) are $m_{\text{low}} = 0.0044$ and $m_{\text{high}} = 0.0074$.

Population declines over the course of the experiment were best fit by exponential decline in λ (MLE: $k_0 = 0.13$ [95% confidence interval = 0.118–0.145], $k_4 = 0.02$ [0.012–0.030]). In the zero-seed bottles, exponential decline in λ was a better fit than exponential decline in K ($\Delta\text{AIC} = 9.8$); in the four-seed bottles, the fit was only marginally better ($\Delta\text{AIC} = 1.7$). Using exponential decline in K rather than λ in the model had a similar qualitative effect.

Including population decline in λ in the two-patch model resulted in much lower population densities in both zero- and four-seed bottles (fig. 7*A*, 7*B*, *triangles*). Furthermore, increases in migration rate then produced only slight decreases in *Colpidium striatum* population density at high migration rates in zero-seed bottles (and smaller declines in densities in four-seed bottles; fig. 7*A*, 7*B*, *triangles*).

Adding in both exponential decline in λ and differences in cell volume of dispersing individuals (fig. 7*A*, 7*B*, *squares*) produced a similar pattern (but at lower density) to adjusting for cell volume but not declines, that is, causing population densities in the zero-seed bottle to increase then decrease with increasing dispersal rate. However, observed dispersal rates corresponding to increases in the density in zero-seed bottles were still very low compared to the dispersal need to cause peak densities in the model. Adding in negative population trends and cell volumes did, however, produce low average population densities.

Overall, accounting for differences in cell volume for migrants between zero- and four-seed bottles did predict the correct qualitative patterns of *C. striatum* density in zero-seed bottles versus dispersal rate but only at dispersal rates that were much greater than those seen in the dispersal experiment. Additionally, all migration caused declines in mean *C. striatum* density in four-seed bottles, whereas no significant decline was seen in the spatial dynamics experiment (but power was weak). Absolute average densities of *C. striatum* in the spatial dynamics experiment were intermediate between the predictions of models including cell volumes and with or without trends in long-term dynamics (cf. fig. 4 with fig. 7).

Consistent with pseudosink dynamics, all models produced finite growth rates (λ) in the zero-seed bottles that were substantially below 1.0 when immigration was included in dynamics (fig. 7*C*).

Discussion

Our results broadly support the simplistic views of dispersal presented in source-sink models, with a net flux of individuals from high resource to low resource patches (e.g., Pulliam 1988; Howe et al. 1991). However, the emergent effects of movement on dynamics were complex. This system does not fit the expected patterns of abundance in source and sink systems. Pulliam (1988) constructed a model where in a source population all individuals in excess of the carrying capacity dispersed to sink populations. Pulliam's (1988) model predicted that sink populations would be larger when more individuals moved from sources to sinks, which occurred when sources were more productive. By contrast, we found that compared to isolated zero-seed patches without any immigration, zero-seed patches that were connected to four-seed patches by short tubes (permitting substantial immigration; fig. 6*A*) showed *Colpidium striatum* populations that were of similar size, and they declined just as fast (fig. 3; table 3). Furthermore, the average population densities in zero-seed patches were greater with low dispersal than with either high dispersal or no dispersal (fig. 4). This pattern might be explained by several alternative hypotheses: local adaptation, nutrient diffusion, strong density dependence in zero-seed bottles creating pseudosinks, or a decline in the number of emigrants from four-seed bottles.

Local adaptation cannot reasonably account for this pattern (fig. 4). Selection for more efficient resource use should be equivalent in no, low, and high dispersal zero-seed bottles. Considering that gene flow slows local adaptation, no dispersal bottles should be best adapted to

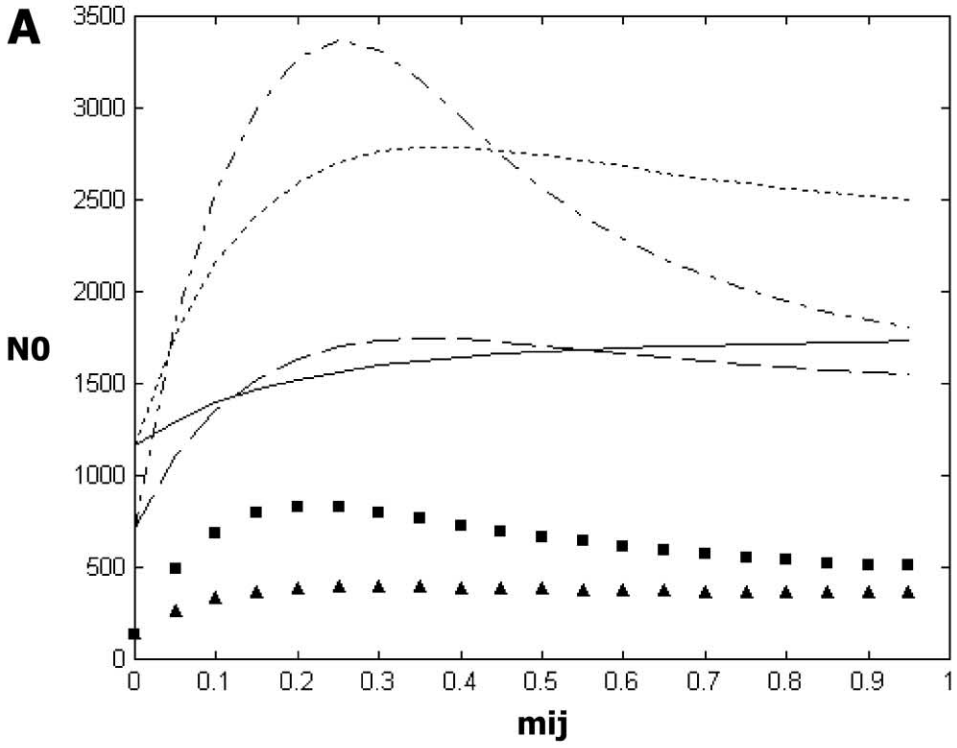
A
N0
mij
0
500
1000
1500
2000
2500
3000
3500
0
0.1
0.2
0.3
0.4
0.5
0.6
0.7
0.8
0.9
1

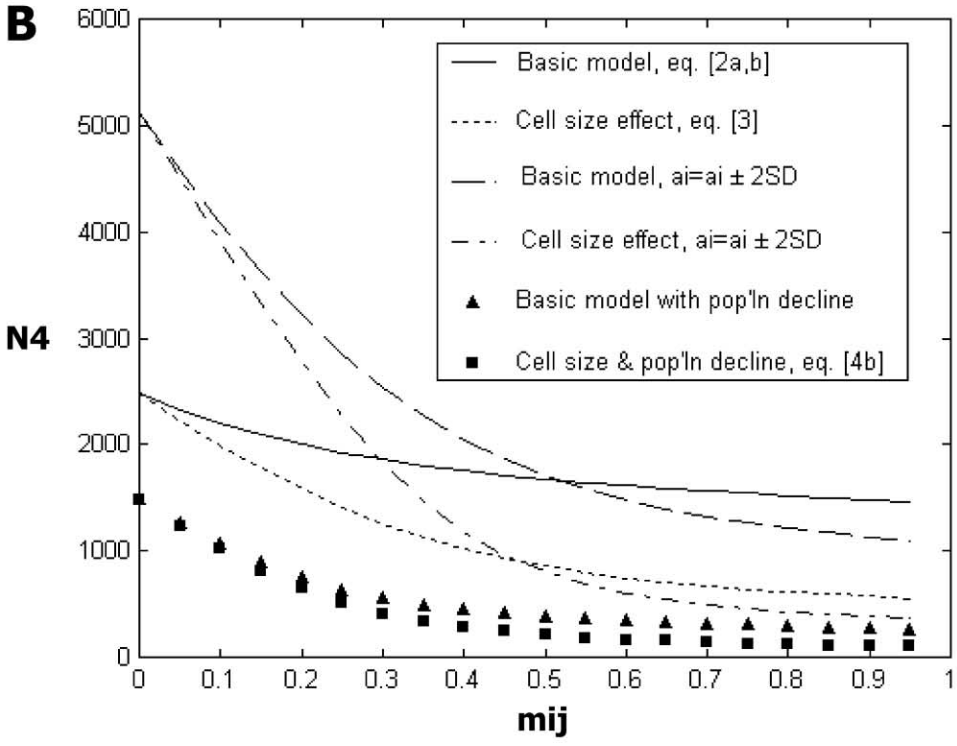
B
N4
mij
Basic model, eq. [2a,b]
Cell size effect, eq. [3]
Basic model, ai=ai ± 2SD
Cell size effect, ai=ai ± 2SD
Basic model with pop'ln decline
Cell size & pop'ln decline, eq. [4b]
0
1000
2000
3000
4000
5000
6000
0
0.1
0.2
0.3
0.4
0.5
0.6
0.7
0.8
0.9
1

low resources and have higher population densities than bottles with dispersal, contrary to our observation (fig. 4).

Nutrient diffusion is also an unlikely explanation for the pattern of *C. striatum* densities (fig. 4). If nutrients are diffusing through the microcosms, *C. striatum* should reflect underlying nutrient distributions (based on observations in isolated bottles). For this to explain our pattern, the nutrient levels in zero-seed bottles would have to be higher in low dispersal bottles than in high or no dispersal bottles. Since dissolved nutrients diffuse more quickly over shorter distances, the nutrients (and, therefore, population densities) should be higher in high dispersal bottles, contrary to our observation.

Since our populations declined over the course of the experiment, there is an alternative nutrient diffusion explanation. Since resources in the four-seed bottles are finite, nutrient levels in the four-seed bottle should decrease as they diffuse to zero-seed bottles. This would attenuate the diffusion gradient between four- and zero-seed bottles and result in a decrease over time in nutrients moving from four- to zero-seed bottles; this effect should be more pronounced in high dispersal microcosms than low dispersal microcosms. Three pieces of information lead us to believe that this cannot explain the pattern we saw: first, there was no significant difference in four-seed average densities between low and high dispersal bottles as you would expect if resources in the four-seed patches were being depleted (fig. 4). Second, if there was a direct relationship between local resource availability and protist density, we would expect total density to be conserved. However, zero-seed bottles with low dispersal had a mean of 704 *C. striatum* mL^{-1} more than with high dispersal, which was not offset by the difference between four-seed low and high dispersal bottles. The actual difference in

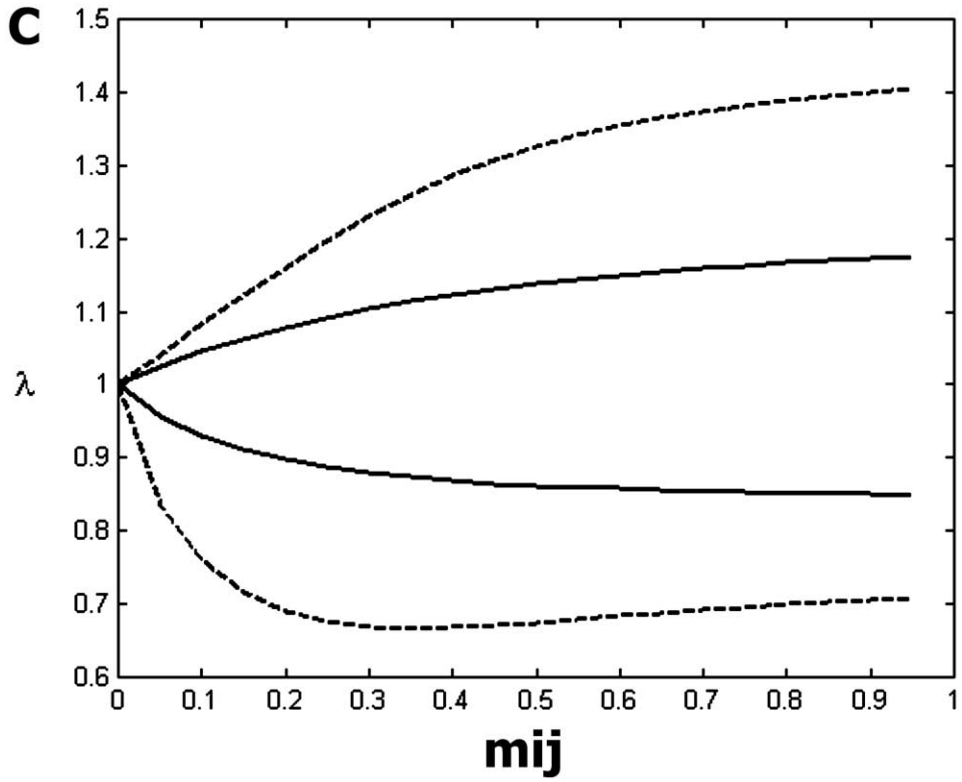

Figure 7: Simulated population densities versus symmetrical per capita dispersal rates ($m_{04} = m_{40}$) in zero-seed (*A*) and four-seed (*B*) patches. *C* is patch growth rate for zero-seed and four-seed patches (lines >1.0 are for the four-seed bottle and lines <1.0 are for the zero-seed bottles). The legend in *B* is for all panels. The solid line is the two-patch Beverton-Holt model (eqq. [2a], [2b]). The dashed line is the two-patch model with a larger difference between low and high resource patches ($a_0 = a_0 + 2\sigma_{a0}$, $a_4 = a_4 - 2\sigma_{a4}$). The dotted line is the two-patch model adjusted for cell size (eq. [3]). The dashed-dotted line is the two-patch model adjusted for cell size (eq. [3]) with the larger difference between resource patches ($a_0 = a_0 + 2\sigma_{a0}$, $a_4 = a_4 - 2\sigma_{a4}$). The triangles indicate the two-patch model (eqq. [2a], [2b]) plus exponential decline in λ (eq. [4b]). The squares are the two-patch model adjusted for both cell size and exponential decline in λ (eq. [4b]). In *C*, only the two-patch model (*solid lines*) and the two-patch model adjusted for cell size (*dashed lines*) are plotted. From the dispersal experiment, the empirical dispersal rates were $m_{low} = 0.0044$ and $m_{high} = 0.0074$.

density in four-seed bottles was only 125 mL^{-1}, which was significantly smaller than if density were conserved (Student's $t_3 = 6.01$, $P < .01$). Third, there is no difference in the rate of decline in four-seed bottles between high and low dispersal patches as you might expect if resources in the four-seed patches were being depleted more quickly in the high dispersal bottles (fig. 3; table 3).

Strong density dependence in zero-seed bottles could explain our pattern (fig. 4). If dispersal changes the zero-seed bottle into a pseudosink, then increasing dispersal could result in a decline in zero-seed bottle densities. While this is a plausible explanation, it cannot explain the pattern we see given the parameter values in our microcosms (fig. 7*A*). Our simulation results indicate that the zero-seed bottle does indeed become a pseudosink ($\lambda < 1$) over a broad range of dispersal rates (fig. 7*C*); however, the effect on λ was not sufficiently strong to account for the observed pattern of densities.

A decrease in the number of emigrants from four-seed bottles could potentially explain the pattern (fig. 4). As individuals emigrate from four-seed bottles, those remaining are released from local regulation and reproduce at the maximum rate. Further increases in emigration cause four-seed bottle densities to decline since local individuals cannot fully utilize local resources; this, in turn, reduces the number of immigrants into zero-seed patches. Watkinson and Sutherland (1995), using a model like ours, demonstrate this but only for very high dispersal rates (0.7). Doak (1995), using a density-independent source-sink model, attributed the decline in total population growth rate (including both good and bad patches) with increasing movement rates to this cause. This result is not dependent on density dependence in the zero-seed bottle: simulations excluding density dependence in the zero-seed bottle gave the same general results as those in figure 7*A*. Using the maximum likelihood demographic rates that we estimated from the perturbation experiment, the relationship between zero-seed bottle density and symmetrical dispersal rate is monotonically increasing (fig. 7*A*, *solid line*), contrary to our observation in the zero-seed bottles. However, by taking cell sizes and/or population decline into account, this explanation becomes plausible, but only at dispersal rates much greater than those observed (fig. 7*A*).

Asymmetry in migration could account for the zero-seed pattern in figure 4. Though we found no difference in the per capita dispersal rate between zero- and four-seed bottles (table 1), asymmetry in cell size between zero- and four-seed bottles results in an asymmetry of biomass dispersal. A strong enough asymmetry (such that m_{40} is higher than m_{04}) can result in a hump-shaped relationship between zero-seed bottle density and dispersal (fig. 7, *dotted line*). This kind of asymmetry in dispersal is akin to the maladaptive habitat selection discussed by Delibes et al. (2001). We accounted for cell size in a nonconservative way (eq. [3]), using fixed size differences between zero- and four-seed bottles estimated from no dispersal bottles (fig. 5). Despite this, including this difference in body size is not enough to account for the empirical relationship between zero-seed bottle density and dispersal rate (fig. 4).

Population decline in addition to asymmetry in migration could help explain our pattern (fig. 4). Increasing the difference between high- and low-quality patches accentuates the hump-shaped relationship between zero-seed bottle density and dispersal (fig. 7*A*, *dashed* and *dotted-dashed lines*). In our system, exponential decline in growth rate was faster in zero-seed bottles than in four-seed bottles; this corresponds to an increasing difference in patch quality between zero- and four-seed bottles over time. Based on parameters at the beginning of the experiment and adjusting dispersal for biomass asymmetry, the relationship between zero-seed patch density and dispersal rate is only slightly hump shaped (fig. 7*A*, *dotted line*); with larger differences between zero- and four-seed patch parameters, this relationship becomes strongly hump shaped (fig. 7, *dashed-dotted line*). However, the overall decline in population size swamps the effect of this increasing deviation in demographic rates between zero- and four-seed bottles (fig. 7, *triangles* and *squares*).

In our consideration of these alternative hypotheses, our lack of information about microbial processes becomes problematic. We have little data on the movement of resources both during protist dispersal and by diffusion, potential feedbacks between within-patch protist population densities and resource levels for bacterial growth, and release and recycling of nutrients by *C. striatum* and bacteria. While we have found qualitative agreement between this simple model and our data, we do not find quantitative agreement with our empirical results, even in this simple system.

Dispersal in these microcosms did not fit the idea of balanced dispersal (McPeek and Holt 1992) or optimal foraging (Fretwell and Lucas 1970), which would predict no net flux of individuals (or biomass) between high and low resource patches. McPeek and Holt (1992) examined a model with two patches with different carrying capacities. They showed that per capita emigration rates should evolve to become inversely related to donor patch carrying capacity, such that there was no net flux of individuals between patches. However, this assumes that there is no cost to movement, that individuals have perfect knowledge of resource availability in different patches, and that the timescale of movement is short relative to that of within-patch dynamics. Violation of any of these assumptions might explain the net flux of individuals observed here.

Our results can also contribute to knowledge about

source-sink inversions. Existing studies have demonstrated that changes in patch occupancy can cause sources to become sinks (Dias 1996; Boughton 1999). The observed reduction in the difference in density between high and low resource patches during our experiment is not as extreme as a source-sink inversion but is a related phenomenon. Increases in *C. striatum* cell volumes also indicated that nutrient transportation was associated with this phenomenon. This could be an example of changes in relative source and sink status through a form of subsidy—the effect of transport of materials from one ecosystem (location) to another (Polis et al. 1997; Stapp et al. 1999). In the present case, this is complicated because when protists moved between bottles, their feeding would be expected to release nutrients back into the solution, which might then fuel bacterial population growth (Sambanis and Fredrickson 1988; Jaworska et al. 1996; Thingstad et al. 1999). Such feedbacks between nutrient release by grazers and the attraction of grazers to higher nutrient areas were also identified by McNaughton et al. (1997) for mammalian herbivores in the Serengeti of Tanzania. Whether there is a net long-term nutrient flux depends on the balance between rates of transport and consumption.

In conclusion, our results demonstrate that while source-sink models predict net fluxes of individuals (e.g., Pulliam 1988; Howe et al. 1991), other aspects of dynamics were not adequately explained by these models. Source-sink, pseudosink, and balanced dispersal models were all incapable of predicting the long-term dynamics in even these relatively simple systems. The magnitude of the net flow of individuals depended on the dispersal treatment in the expected ways, but the responses of within-patch populations to this dispersal were counterintuitive, with lower densities in higher dispersal microcosms. Modeling indicated that asymmetrical dispersal and/or increasing differences between high and low resource patches could account for this effect but not at the low observed rates of dispersal. Furthermore, the flow of individuals did not exactly predict the flow of biomass (fig. 6*B*), which also depended on who moved (fig. 5). Interpatch movement also changed the net state of individuals, measured through body size. Further work is required to quantify and understand the complex feedbacks between movement and within-patch dynamics.

Acknowledgments

We thank P. Chesson, J. Fox, B. Kendall, S. P. Lawler, and an anonymous referee for comments. We appreciate the support of B. Hope and R. Pomeroy of the University of California, Davis, Young Scholar's Program (YSP). This project was supported by National Science Foundation (NSF) DEB 96-29876 to M.H. and S. Harrison. M.J.D. was supported during analysis and writing by a dissertation fellowship from the American Association of University Women and NSF DBI-9602226 (research training grant for nonlinear dynamics in biology) awarded to the University of California, Davis. C.F.'s involvement was supported by the YSP.

Literature Cited

Beverton, R. J. H., and S. J. Holt. 1957. On the dynamics of exploited fish populations. U.K. Ministry of Agriculture and Fisheries, Fisheries Investigations, ser. 2, vol. 19.

Boughton, D. A. 1999. Empirical evidence for complex source-sink dynamics with alternative states in a butterfly metapopulation. Ecology 80:2727–2739.

Burnham, K. P., and D. R. Anderson. 1998. Model selection and inference: a practical information-theoretic approach. Springer, New York.

Cain, M. L. 1991. When do treatment differences in movement behaviors produce observable differences in long-term displacements? Ecology 72:2137–2142.

Cohen, J. 1988. Statistical power analysis for the behavioral sciences. 2d ed. Erlbaum, Hillsdale, N.J.

Delibes, M., P. Gaona, and P. Ferreras. 2001. Effects of an attractive sink leading into maladaptive habitat selection. American Naturalist 158:277–285.

Dennis, B., and M. Taper. 1994. Density dependence in time series observations of natural populations: estimation and testing. Ecological Monographs 64:205–224.

Dias, P. C. 1996. Sources and sinks in population biology. Trends in Ecology & Evolution 11:326–330.

Diffendorfer, J. E. 1998. Testing models of source-sink dynamics and balanced dispersal. Oikos 81:417–433.

Doak, D. F. 1995. Source-sink models and the problem of habitat degradation: general models and applications to the Yellowstone grizzly. Conservation Biology 9: 1370–1379.

Finlay, B. J. 1977. The dependence of the reproductive rate on cell size and temperature in freshwater protozoa. Oecologia (Berlin) 30:75–81.

Fretwell, S. D., and H. L. Lucas. 1970. On territorial behavior and other factors influencing habitat distributions in birds. Acta Biotheoretica 19:16–36.

Hewett, S. W. 1980. The effect of prey size on the functional and numerical responses of a protozoan predator to its prey. Ecology 61:1075–1081.

Hilborn, R., and M. Mangel. 1997. The ecological detective: confronting models with data. Princeton University Press, Princeton, N.J.

Holyoak, M. 2000. Habitat subdivision causes changes in food web structure. Ecology Letters 3:509–515.

Holyoak, M., and S. P. Lawler. 1996*a*. Persistence of an

extinction-prone predator-prey interaction through metapopulation dynamics. Ecology 77:1867–1879.

———. 1996*b*. The role of dispersal in predator-prey metapopulation dynamics. Journal of Animal Ecology 65:640–652.

Howe, R. W., G. J. Davis, and V. Mosca. 1991. The demographic significance of sink populations. Biological Conservation 57:239–255.

Ims, R. A., and N. G. Yoccoz. 1996. Studying transfer processes in metapopulations: emigration, migration and colonization. Pages 247–265 *in* I. Hanski and M. E. Gilpin, eds. Metapopulation dynamics: ecology, genetics and evolution. Academic Press, New York.

Jaworska, J. S., T. G. Hallam, and T. W. Schultz. 1996. A community model of ciliate *Tetrahymena* and bacteria *E. coli*: individual-based models of *Tetrahymena* and *E. coli* populations. Pt. 1. Bulletin of Mathematical Biology 58:247–264.

Kaunzinger, C. M. K., and P. J. Morin. 1998. Productivity controls food-chain properties in microbial communities. Nature 395:495–497.

McNaughton, S. J., F. F. Banyikwa, and M. M. McNaughton. 1997. Promotion of the cycling of diet-enhancing nutrients by African grazers. Science 278:1798–1800.

McPeek, M. A., and R. D. Holt. 1992. The evolution of dispersal in spatially and temporally varying environments. American Naturalist 140:1010–1027.

Monod, J. 1950. La technique de la culture continue: theorie et applications. Annales de l'Institut Pasteur 79: 390–410.

Nakano, S., and M. Murakami. 2001. Reciprocal subsidies: dynamic interdependence between terrestrial and aquatic food webs. Proceedings of the National Academy of Sciences of the USA 98:166–170.

Polis, G. A., W. B. Anderson, and R. D. Holt. 1997. Toward an integration of landscape and food web ecology: the dynamics of spatially subsidized food webs. Annual Review of Ecology and Systematics 28:289–316.

Pulliam, H. R. 1988. Sources, sinks, and population regulation. American Naturalist 132:652–661.

———. 1996. Sources and sinks: empirical evidence and population consequences. Pages 45–69 *in* O. E. Rhodes, Jr., R. K. Chesser, and M. H. Smith, eds. Population dynamics in ecological space and time. University of Chicago Press, Chicago.

Sambanis, A., and A. G. Fredrickson. 1988. The persistence of bacteria in the presence of viable, nonencysting, bacterivorous ciliates. Microbial Ecology 16:197–211.

Stapp, P., G. A. Polis, and F. Sanchez Pinero. 1999. Stable isotopes reveal strong marine and El Niño effects on island food webs. Nature 401:467–469.

Thingstad, T. F., H. Havskum, H. Kaas, T. G. Nielsen, B. Riemann, D. Lefevre, and P. J. L. B. Williams. 1999. Bacteria-protist interactions and organic matter degradation under P-limited conditions: analysis of an enclosure experiment using a simple model. Limnology and Oceanography 44:62–79.

Tilman, D. 1977. Resource competition between planktonic algae: an experimental and theoretical approach. Ecology 58:686–692.

———. 1982. Resource competition and community structure. Princeton Monographs in Population Biology. Princeton University Press, Princeton, N.J.

Watkinson, A. R., and W. J. Sutherland. 1995. Sources, sinks and pseudo-sinks. Journal of Animal Ecology 64: 126–130.

Wootton, J. T., and D. A. Bell. 1992. A metapopulation model of the peregrine falcon in California: viability and management strategies. Ecological Applications 2: 307–321.

Associate Editor: Daniel F. Doak